Journal of Advanced Scientific Research

Available online through http://www.sciensage.info

ISSN
0976-9595
Research Article

BINARY FISSION OF SUPERHEAVY NUCLEI ^{299}121

N. Manjunatha*[1,2], N. Sowmya[1], H.C. Manjunatha[1], P.S. Damodara Gupta[1], T. Ganesh[3]

[1]*Department of Physics, Government College for Women, Kolar, Karnataka, India*

[2]*Department of Physics, Rajah Serfoji Government College, Thanjavur, Affiliated to Bharathidasan University, Tiruchirappalli, TamilNadu*

**Corresponding author: manjunathhc@rediffmail.com*

ABSTRACT

The binary fission of superheavy nuclei ^{299}121 and fission fragments is studied using Coulomb and proximity potential model. The total potential is evaluated using the recent proximity potential model. The total potential is evaluated for different fission fragment combinations. The probable fission fragment combination has been obtained using a cold valley plot. The identified favourable fission fragments are found to be ^{139}La+$^{160-166}$Gd with the half-life in the order less than zeptoseconds. The role of symmetric or asymmetric fission fragments were analysed. The binary fission fragment combination ^{139}La+^{160}Gd with maximum yield and smaller half-lives in which the fission fragment ^{139}La will have magic neutron number with N=82.

Keywords:

1. INTRODUCTION

Elements with $Z \geq 104$ are called as superheavy elements, synthesized by cold and hot fusion reactions during past few decades [1]. Superheavy elements are less stable because of large number of protons and neutrons, therefore they undergo α-decay, β-decay or spontaneous fission [2] resulting in the formation of fission fragments. The structure of the superheavy elements depends on binding energies, shell effects, proton and neutron states [3].

In general, during the spontaneous fission process, the unstable nucleus splits into two binary fission (BF) fragments of similar masses. It is well known that the properties of fission fragments vary considerably with the number of protons and neutrons of the fissioning nuclei. The fission yield of ^{256}Fm by spontaneous fission exhibit asymmetric behaviour [4,5]. However, contradictory results were observed in dominant decay mode of ^{257}Fm [6, 7]. Earlier researchers [10-13] were studied BF fragments of heavy and superheavy nuclei. Based on quantum mechanical fragmentation theory (QMFT), Sharma et al., [14] studied binary and ternary fission in ^{253}Es.

Pahlavani and Joharifard [15] studied half-lives and isotopic yield of spontaneous fission in superheavy nuclei ^{280}Ds and ^{282}Cn. Sharma et al., [16] theoretically studied spontaneous fission and competing decay mode in tranactinide and actinide. Rundrup et al., [17] theoretically studied spontaneous fission half-lives using semi-empirical WKB framework in even nuclei with Z≥92. Nilsson et al., [18] Using spontaneous fission half-lives near Z=114 and N=184, quadrupole and hexadecapole distortion were reported. Earlier researchers [19-27] studied different decay modes such as cluster-decay, proton-decay, an alpha-decay and spontaneous fission in the heavy and superheavy nuclei. The limited studies on spontaneous fission has motivated us to investigate possible BF fragments in the superheavy nuclei ^{299}121.

The Section II gives a complete description of theory used to evaluate and identification of probable fission fragments. Section III describes the results and discussion corresponding to theory used to study BF in superheavy nuclei ^{299}121. Conclusions presented in Section 4.

2. THEORY

The total potential during BF is a sum of Coulomb and proximity potential

$$V = V_{Nij}(R) + V_{Cij}(R) \quad (1)$$

The Coulomb potential V_{Cij} is defined as;

$$V_{Cij}=\begin{cases}\dfrac{Z_iZ_je^2}{R_{ij}} & \mathrm{R}_{ij}\geq R_i+R_j,\\ \dfrac{Z_iZ_je^2}{R_{ij}}\Delta & R_i-R_j\leq R_{ij}\leq R_i+R_j\\ Z_iZ_je^2\lambda & R\leq R_{ij}\leq R_i-R_j\end{cases} \tag{2}$$

with [28]

$$\Delta=\left[1-\frac{\left(R_i+R_j-R_{ij}\right)^4\Delta_1}{160R_i^3R_j^3}\right] \tag{3}$$

$$\Delta_1=R_{ij}^2+4R_{ij}(R_i+R_j)+20R_iR_j-5R_i^2-5R_j^2 \tag{4}$$

$$\lambda=\frac{15R_i^2-3R_j^2-5R_{ij}^2}{10R_i^3} \tag{5}$$

where R_{ij} is the separation distance between two fragments. The short-range nuclear potential is defined as ;

$$V_{Pij}(Z)=4\pi\gamma b\overline{R}_{ij}\Phi\left(\frac{z}{b}\right) \tag{6}$$

where $\overline{R}=\dfrac{R_1R_2}{R_1+R_2}$ is the mean radius of curvature. In the above equation, γ is the specific nuclear surface tension and it is given by

$$\gamma=\gamma_0\left[1-K_S\left(\frac{N-Z}{A}\right)^2\right]\quad \mathrm{MeV/fm^2} \tag{7}$$

where $\gamma_0=$ 1.460734 and K_s=4.0. The universal proximity potential Φ in equation (6) is as a function of distance between the near surfaces of the fragments (z) and nuclear surface thickness b=0. In the present work, we have used the following universal function $\Phi(\varepsilon=z/b)$ is defined as;

$$\Phi(\varepsilon)=\begin{cases}-4.41\exp\left(\dfrac{-\varepsilon}{0.7176}\right) & \text{for} 0\leq\varepsilon\leq 1.9475\\ -1.7817+0.9270\varepsilon+0.0169\varepsilon^2-0.05148\varepsilon^3 & \text{for} 0\leq\varepsilon\leq 1.9475\end{cases} \tag{8}$$

The radius of each fragment in equation (6) is defined as;

$$R_i=1.28A_1^{1/3}-0.76+0.8A_2^{-1/3} \tag{9}$$

For process such as BF, the barrier penetrability P is given as [29]

$$P=\exp\left\{-\frac{2}{\hbar}\int_a^b\sqrt{2\mu(V-Q)}dz\right\} \tag{10}$$

Here $\mu=A_1A_2/A$, For fission process, first and second turning point is determined from the equation $V(a)=V(b)=Q$. The half-lives of BF fragments are evaluated by

$$T_{1/2}=\frac{\ln 2}{\lambda}=\frac{\ln 2}{\upsilon P} \tag{11}$$

where υ is assaults frequency, in case of BF [30].

$$\upsilon=\frac{\sqrt{2Q/\mu}}{2(C_1+C_2)} \tag{12}$$

where C_1 and C_2 are the Scissmann radii of the BF fragments.

3. RESULTS AND DISCUSSION

The total potential is evaluated using the long range Coulomb force and short range nuclear force. The total potential is taken as sum of Coulomb potential and proximity potential. The universal function play a major role in the evaluation of nuclear potential. The Fig. 1 shows the variation of (a) Coulomb, (b) nuclear and (c) total potential as function of fission fragment mass A_1. From the Fig. 1(a) it has been observed that as the mass number of fission fragment increases Coulomb potential also increases. Similarly, Fig. 1(b) shows the variation of nuclear potential as function of A_1. The nuclear potential is maximum for A_1=71 and it gradually decreases with increase in mass number. The value of short range forces gradually decreases with increase in number of nucleons in which Colombian repulsive force is more dominant. The total potential as a sum of Coulomb and nuclear potential is gradually increases with mass number of fission fragment. The value of Coulomb potential is more dominant when compared to nuclear potential in the superheavy nuclei ^{299}121. Then, the driving potential is evaluated using amount of energy released during the BF. The amount of energy released during the fission process is the difference between mass excess of parent nuclei and mass excess of fission fragments. These mass excess values have been taken from the reference [31-35].

Then, we have evaluated penetration probability using WKB integral. The penetration probability is the area under the curve of driving potential as a function of separation distance between the two nuclei. The Fig. 2 depicts the variation of penetration probability as function of fission fragment mass number A_1. The penetration probability is maximum for the fission fragment combination ^{86}Kr+^{213}At, ^{133}Cs+^{166}Dy, ^{139}La+^{160}Gd and ^{140}Ce+^{159}Eu when compared to their neighbouring fission fragment combination. The maximum penetration probability is observed due to their shell closures and which are also near magic or semi magic nuclei. In case of ^{86}Kr+^{213}At fission fragment combination ^{86}Kr is having Z=36 and N=50, where ^{86}Kr is having magic number of N=50. Similarly, ^{166}Dy (N=100), ^{139}La (N=82) and ^{140}Ce (N=82) are having magic number due to which the penetration probability is having maximum value when compared to their neighbouring ones. From this fission fragment combination it has been observed that the combination ^{86}Kr+^{213}At is asymmetric and other three combinations such as ^{133}Cs+^{166}Dy, ^{139}La+^{160}Gd and ^{140}Ce+^{159}Eu are almost symmetric fission combination with larger penetration probability.

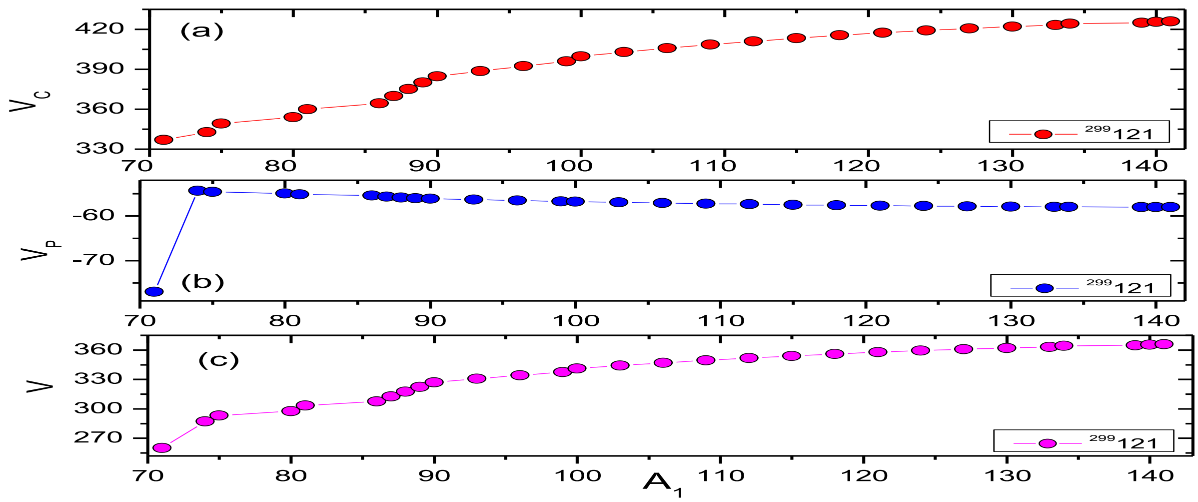

Fig. 1: The variation of (a) Coulomb, (b) nuclear and (c) total potential as function of fission fragment mass A_1

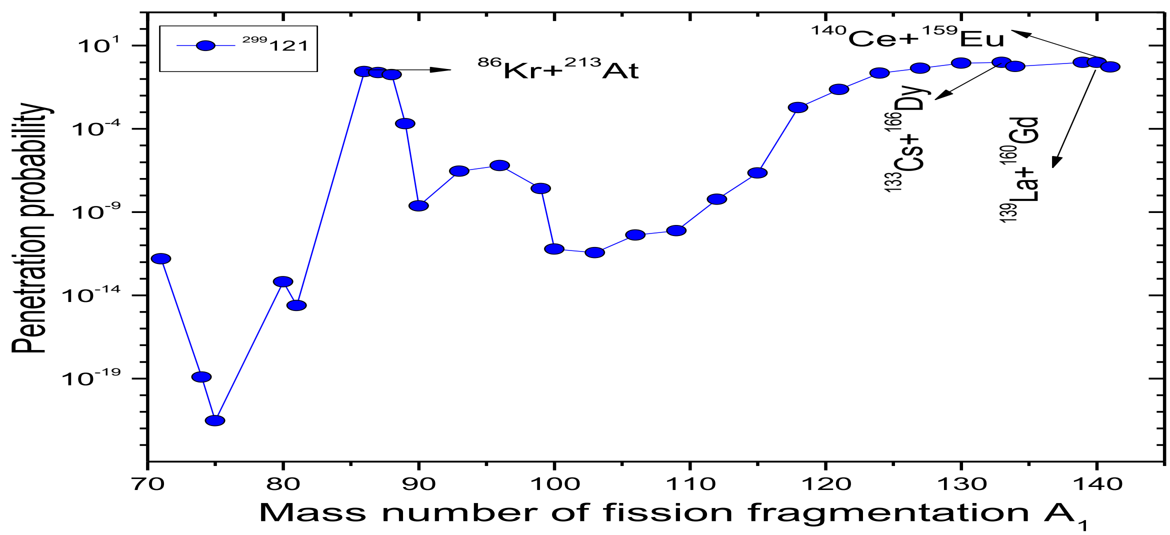

Fig. 2: The variation of penetration probability as a function of mass number of fission fragment A_1

The Fig. 3 depicts the variation of logarithmic half-lives as function of fission fragment mass number A_1. As similar to relative yield, the $\log T_{1/2}$ is minimum for the fission fragment combination ^{86}Kr+^{213}At, ^{133}Cs+^{166}Dy, ^{139}La+^{160}Gd and ^{140}Ce+^{159}Eu when compared to their neighbouring fission fragment combination. Among these, the minimum logarithmic half-lives are observed for the fission fragment combination La+Gd with N=82 for Lanthanum in superheavy nuclei ^{299}121. The predicted half-lives for possible fission fragment combination are less than zeptoseconds. From the analysis, it has been observed that the fission fragment combination with magic number of neutron shows smaller half-lives and larger relative yield.

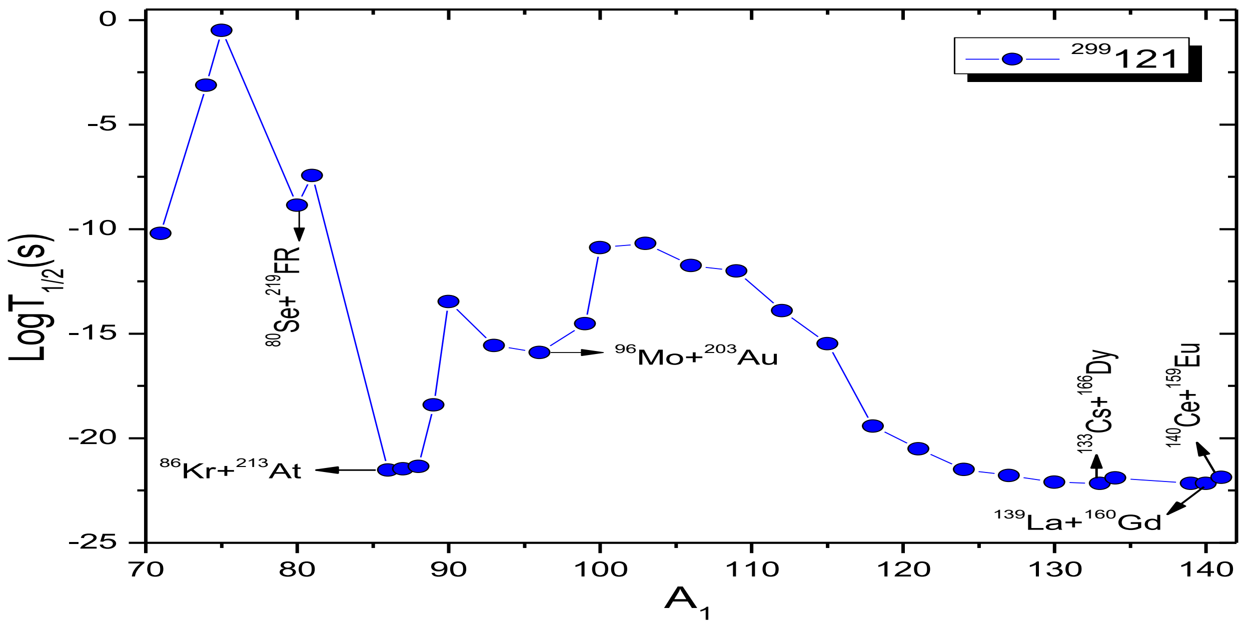

Fig. 3: The variation of logarithmic half-lives as a function of mass number of fission fragment A_1

4. CONCLUSIONS

We studied BF of superheavy nuclei $^{299}121$ using Coulomb and proximity potential model. The penetration probability is maximum for the fission fragment combination La+Gd with N=82. The asymmetric combination of fission fragment combination produces larger relative yield and smaller half-lives lesser than zeptoseconds. Hence, ^{139}La+$^{160-166}$Gd are possible BF fragment combinations with maximum yield and smaller half-lives in which the fission fragment ^{139}La posses magic neutron number with N=82.

5. REFERENCES

1. Giuliani SA, Matheson Z, Nazarewicz W, Olsen E, et al. *Rev Mod Phys*, 2019; **91**:011001.
2. Nilsson SG, Tsang CF, Sobiczewski A, Szyma ́nski Z, et al. *Nucl Phys A*, 1969; **131**:1.
3. Cwiok S, Dobaczewski J, et al. *Nucl Phys A,* 1996*;* **611**:211.
4. Flynn KF, Horwitz EP, Bloomquist CAA, Barnes RF, Sjoblom RK, Fields PR, Glendenin LE. *Phys Rev C,* 1972*;* **5**:1725.
5. Bemis CE, Ferguson RL, Plasil F, Silva RJ, OKelley GD, Kiefer ML, et al. *Phys Rev Lett*, 1977;**39**:1246.
6. Balagna JP, Ford GP, Hoffman DC, Knight JD. *Phys Rev Lett*, 1971; **26**:145.
7. Sowmya N, Manjunatha HC. *Braz J Phys*, 2019; **49**: 874-886.
8. Manjunatha HC, Sowmya N. *Int J Appl Phys*, 2018; **9**:79-82.
9. John W, Hulet EK, Lougheed RW, Wesolowski JJ. *Phys Rev Lett*, 1971; **27**:45.
10. Manjunatha HC, Sowmya N. *Int J Mod Phys E*, 2018; **27(5)**:1850041.
11. Manjunatha HC, Sridhar KN, Sowmya N. *Phys Rev C,* 2018*;* **98**:024308.
12. Sowmya N, Manjunatha HC. *Bulg J Phys,* 2019*;* **46**:16-27.
13. Manjunatha HC, Sowmya N, *Nucl Phys A*, 2018; **969**:68-82.
14. Nitin Sharma, Amandeep Kaur, Manoj K, Sharma, *Phys Rev C*, 2020; **102**:064603.
15. Pahlavani MR, Joharifard M. *Eur Phys J* A, 2018; **54**:171.
16. Sharma K, Sawhney, Sharma MK, *Phys Rev C*, 2017; **96**:054307.
17. Randrup J, Larsson SE, Möller P, Nilsson SG, et al. *Phy Rev C*, 1976;**13**: 229.
18. Nilsson SG, Nix JR, Sobiczewski A, Szymański Z, et al. *Nucl Phys A*,1968;**115**:3, 545-562.
19. Manjunatha HC, Sowmya N. *J Radioanal Nucl Chem*, 2017; **314**, 2, 991-999.
20. Sowmya N, Manjunatha HC. *Braz J Phys,* 2019; **49**: 874.
21. Srinivas MG, Manjunatha HC, Sridhar KN, Sowmya N, Alfred Cecil Raj. *Nucl Phys A*, 2020; **995**:1216.

22. Sridhar GR, Manjunatha HC, Sowmya N, Damodara Gupta PS, Ramalingam HB. *Eur Phys J Plus*, 2020; **135**:291.
23. Sowmya N, Manjunatha HC. *Braz J Phys*, 2020; **50**:317-330.
24. Sowmya N, Manjunatha HC. *Phys Part Nucl*, 2020; **17(3)**:370-378.
25. Manjunatha HC, Sowmya N, Manjunatha N, Seenappa L. *Int J Mod Phys E* , 2020;**29(5)**:2050028.
26. Nagaraja AM, Manjunatha HC, Sowmya N, Manjunatha N, Alfred Cecil Raj S. *Eur Phys J Plus,* 2020*;* **135**:814.
27. Nagaraja AM, Manjunatha HC, Sowmya N. *J Nucl Phys Mat Sci Rad A*, 2020;**8(1)**:55-63.
28. Kermode MW, Mustafa MM, Rowley N. *J Phys G Nucl Part Phys*, 1990; **16**:299.
29. Zhang HF, Royer G. *Phys Rev C*, 2008; **77**:054318.
30. de Carvalho HG, Martins JB, Tavares OAP, *Phys Rev C*,1986; **34**:2261.
31. Audi G, Wapstra AH. *Nucl Phys A*, 1995; **595**:409.
32. Möller P, Sierk AJ, Ichikawa T, Sagawa H. *At Dat Nucl Dat Tables,* 2016; **109**.
33. Manjunatha HC, Chandrika BM, Seenappa L. *Mod Phys Lett A,* 2016; **31(28)**:1650162.
34. Wang M, Audi G, Wapstra AH, et al. *Chin Phys C*, 2012; **36**:1603.
35. Manjunatha HC, Sowmya N. *Mod Phys Lett A*, 2019; **34 (15)**:1950112.